GANIT

Available online at https://ganitjournal.bdmathsociety.org/

GANIT: Journal of Bangladesh Mathematical Society

GANIT *J. Bangladesh Math. Soc.* 41.2 (2021) 41–52
DOI: https://doi.org/10.3329/ganit.v41i2.57573

Study on Magnetohydrodynamics Cu-water Nanofluid Flow with Different Shapes of Nanoparticles in a Divergent Channel

Md. Sarwar Alam*, Suraiya Yasmin, and Ashik Chandra Das

Department of Mathematics, Jagannath University, Dhaka-1100, Bangladesh

ABSTRACT

This paper studies the two-dimensional magnetohydrodynamics steady incompressible Cu-water nanofluid flow considering different shapes of nanoparticles in a divergent channel. The continuity equation, momentum equations and energy equation governing the problem are transformed to a set of non-dimensional ordinary differential equations by suitable transformations. The transformed dimensionless equations are solved by using power series approach and then Hermite-Padé approximation method is applied for analyzing the solution. Brick, cylinder and platelet-shaped Cu-nanoparticles are considered to investigate the effect of shape factor. Moreover, impact of physical parameters such as channel angle, flow Reynolds number, Hartmann number, Eckert number, Prandtl number and nanoparticles solid volume fraction on velocity and temperature profiles are also examined. The results show that the different shapes of Cu-nanoparticles have significant effect on the temperature distributions in the channel.

Received: June 17, 2021 **Accepted:** August 05, 2021 **Published Online:** January 07, 2022

Keywords: Magnetohydrodynamics; Cu-water nanofluid; shape factors; divergent channel; Hermite-Padé approximation.

1. Introduction

Jeffery [1] and Hamel [2] discovered two dimensional viscous incompressible fluid flow in a channel with non-parallel walls. This flow is separated by a fixed angle and moved by a source or sink at a peak which is known as the classical Jeffery-Hamel flow. Many researchers [3-8] have investigated this flow considering various effects such as megnetohydrodynamics (MHD) and heat transfer phenomena through convergent-divergent channels. These flows have the similarity solution of Navier-Stokes equation and the dimensionless parameters are depended on the flow Reynolds number and channel angular width [9]. This type of flows has several applications in industrial, aerospace, chemical, civil, environmental, mechanical and biomechanical engineering.

Magnetohydrodynamics (MHD) is related to the mutual interaction of fluid flow and magnetic field. Many natural and man-made flows are influenced by magnetic field. The theory of megnetohydrodynamics (MHD) states that the presence of magnetic field produces a current through a moving conductive fluid. This inclined

* Corresponding author: Md. Sarwar Alam, *E-mail address:* sarwardu75@gmail.com

current results force on ions of the conductive fluid. The investigation of MHD flow through convergent-divergent channels is not only interesting theoretically but also becomes more applications in mathematical modeling of several industries to design cooling system with liquid metals, MHD generators, accelerators, pumps and flow meters

New types of fluids need to develop, which are more effective in terms of heat exchange performance considering the recent demands of modern technology, including chemical production, power station and microelectronics. Presently, it is seen that the thermal conductivity of fluids has been enhanced with nanoparticles by Choi [10]. Nanoparticles have unique chemical and physical properties and have better thermal conductivity and radiative heat transfer compared to the base fluid only. Nanofluids are engineered dilute colloidal dispersions of nanosized (less than 100 nm) particles in a base fluid such as water, oil and ethylene glycol analysed by Das et al. [11]. These nanoparticles are good conductors of heat and enable the basic fluids to enhance their thermal properties.

An extension of the classical Jeffery-Hamel flows to magnetohydrodynamics was studied by Makinde and Mhone [12]. They explained that the effect of external magnetic field works as a parameter in the solution of magnetohydrodynamics flows in convergent-divergent channels. Makinde and Mhone [13] investigated the terrestrial development of small disturbances in magnetohydrodynamics Jeffery-Hamel flows. This concept described at very small magnetic Reynolds number Rm for the stability of hydromagnetic steady flows in convergent-divergent channels using Chebyshev spectral collocation method. Moradi et al. [14] described the effects of heat transfer and viscous dissipation on the Jeffery-Hamel flow of nanofluids. Alam et al. [15-16], Alam and Khan [17] studied MHD Jeffery-Hamel nanofluid flow for different nanoparticles.

Recently, the effect of nanoparticle shapes on irreversibility analysis of nanofluid flow in a microchannel with radiative heat flux and convective heating was investigated by Sindhu and Gireesha [18]. Asifa et al. [19] performed a comparative fractional study of the significance of shape factor in heat transfer performance of molybdenum-disulfide nanofluid in multiple flow. Moreover, the effects of nanoparticle shape and size on the thermohydraulic performance of plate evaporator using hybrid nanofluids was analysed by Bhattad and Sarkar [20]. Furthermore, Das and Alam [21] investigated different shaped Al_2O_3 and TiO_2 nanoparticles on water-based MHD nanofluid flow through convergent-divergent channels.

To the best of Author's knowledge, the shape factors effect of Cu-water nanofluid flow in divergent channel is not available in open literature yet. This study aims to investigate magnetohydrodynamics Cu-water nanofluid flow in a divergent channel with the effects of three different shapes of nanoparticles; brick, cylinder and platelet. The impacts of various physical parameters namely channel angle α, Reynolds number *Re*, Hartmann number *Ha*, Eckert number *Ec*, Prandtl number *Pr* and nanoparticle solid volume fraction ϕ on velocity profiles and temperature distributions are also discussed.

2. Mathematical Formulation

Consider a two-dimensional viscous incompressible Cu-water nanofluid flow from a source or sink between two channel walls intersect at an angle 2α as seen in Fig.2.1. A cylindrical coordinate system (r, φ, z) is used and the velocity is considered to be purely radial such that it depends on r and φ only. Thus there is no variation for the physical parameters along the z direction. The velocity field takes the form $V = [u(r,\varphi), 0, 0]$. An external magnetic field B_0 is operated vertically downward to the top wall. Let α be the semi-angle and the domain of the flow be $-|\alpha| < \varphi < |\alpha|$. The continuity equation, momentum equations and energy equation with viscous dissipation and Joule heating in reduced polar coordinates are

$$\frac{\rho_{nf}}{r}\frac{\partial}{\partial r}\big(ru(r,\varphi)\big) = 0, \tag{2.1}$$

$$u(r,\varphi)\frac{\partial u(r,\varphi)}{\partial r} = -\frac{1}{\rho_{nf}}\frac{\partial p}{\partial r} + v_{nf}\left(\frac{\partial^2 u(r,\varphi)}{\partial r^2} + \frac{1}{r}\frac{\partial u(r,\varphi)}{\partial r} + \frac{1}{r^2}\frac{\partial^2 u(r,\varphi)}{\partial \varphi^2} - \frac{u(r,\varphi)}{r^2}\right) - \frac{\sigma_{nf}B_0^2}{\rho_{nf}r^2}u(r,\varphi) \tag{2.2}$$

$$\frac{1}{\rho_{nf}r}\frac{\partial p}{\partial \varphi} - \frac{2v_{nf}}{r^2}\frac{\partial u(r,\varphi)}{\partial \varphi} = 0, \tag{2.3}$$

$$u(r,\varphi)\frac{\partial \overline{T}(r,\varphi)}{\partial r}=\frac{\kappa_{nf}}{\left(\rho c_p\right)_{nf}}\left(\frac{\partial^2 \overline{T}(r,\varphi)}{\partial r^2}+\frac{1}{r}\frac{\partial \overline{T}(r,\varphi)}{\partial r}+\frac{1}{r^2}\frac{\partial^2 \overline{T}(r,\varphi)}{\partial \varphi^2}\right)+$$

$$\frac{\mu_{nf}}{\left(\rho c_p\right)_{nf}}\left(4\left(\frac{\partial u(r,\varphi)}{\partial r}\right)^2+\frac{1}{r^2}\left(\frac{\partial u(r,\varphi)}{\partial \varphi}\right)^2\right)+\frac{\sigma_{nf}B_0^2}{\left(\rho c_p\right)_{nf}r^2}\left(u(r,\varphi)\right)^2 \tag{2.4}$$

The respective boundary conditions for the problem are as follows

$$\psi=\frac{Q}{2},\ \frac{\partial \psi}{\partial \varphi}=0 \ \text{ at } \varphi=\pm\alpha$$

$$\overline{T}=T_h \ \text{ at } \varphi=\alpha \ \text{ and } \overline{T}=T_c \ \text{ at } \varphi=-\alpha \tag{2.5}$$

where $\psi=\psi(r,\varphi)$ be the stream function and $\frac{\partial \psi}{\partial \varphi}=ur$. The volumetric flow rate through the channel is defined by

$$Q=\int_{-\alpha}^{\alpha} urd\varphi \tag{2.6}$$

Since the flow is symmetrically radial, i.e. $v=0$. Here, B_0 is the electromagnetic induction, u is the velocity along radial direction and p is the fluid pressure. The effective density ρ_{nf}, the effective dynamic viscosity μ_{nf}, the electrical conductivity σ_{nf} and the kinematic viscosity v_{nf} of the nanofluid are given as.

$$\rho_{nf}=\rho_f(1-\phi)+\rho_s\phi, \qquad \mu_{nf}=\frac{\mu_f}{(1-\phi)^{2.5}}, \qquad v_{nf}=\frac{\mu_{nf}}{\rho_{nf}},$$

$$\frac{\sigma_{nf}}{\sigma_f}=1+\left[3\left(\frac{\sigma_s}{\sigma_f}-1\right)\phi\Big/\left(\left(\frac{\sigma_s}{\sigma_f}+2\right)-\left(\frac{\sigma_s}{\sigma_f}-1\right)\phi\right)\right] \tag{2.7}$$

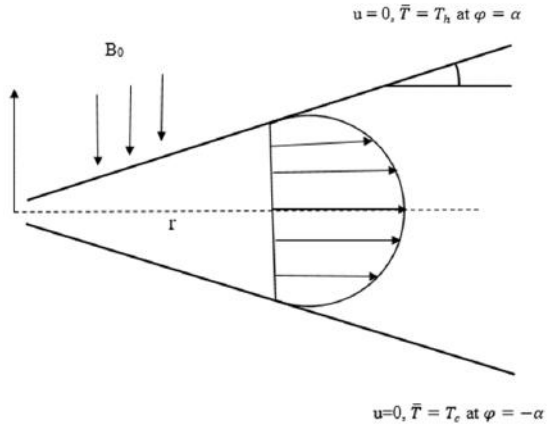

Fig. 2.1: Geometry of the Problem

The corresponding effective thermal conductivity and heat capacity of nanofluid are

$$\kappa_{nf}=\kappa_f\frac{\kappa_s+(m+1)\kappa_f-(m+1)\left(\kappa_f-\kappa_s\right)\phi}{\kappa_s+(m+1)\kappa_f+\left(\kappa_f-\kappa_s\right)\phi},$$

$$(\rho c_p)_{nf} = (1-\phi)(\rho c_p)_f + \phi(\rho c_p)_s \tag{2.8}$$

Here, ϕ is the nanoparticles solid volume fraction and m is the shape factor. The thermophysical properties of water and Cu- nanoparticles as Das et al. [22] are presented in Table 2.1.

Table 2.1: Thermophysical properties of water and Cu-nanoparticles.

Physical properties	Water	Cu
$\rho(kg/m^3)$	997.1	8933
$c_P(J/kgK)$	4179	385
$\kappa(W/mK)$	0.613	401
$\sigma(\Omega m)$	0.05	5.96×10^7

The sphericity and shape factor of Cu-nanoparticles are shown in Table 2.2. As it necessitates $Q \geq 0$, then the flow is diverging from a source at $r = 0$ for $\alpha > 0$.

The dimensionless variable η is introduced as,

$$\eta = \frac{\varphi}{\alpha}$$

Then the dimensionless stream function and temperature are defined by

$$F(\eta) = \frac{2\,\psi(\varphi)}{Q}, \theta(\eta) = \frac{\overline{T} - T_c}{T_h - T_c} \tag{2.9}$$

Table 2.2: Sphericity and shape factor of Cu-nanoparticles [23-25].

Nanoparticle shapes	Aspect ratio	Sphericity	Shape factor
Platelet	1:1/18	0.52	5.7
Cylinder	1:8	0.62	4.9
Brick	1:1:1	0.81	3.7

The pressure term p is eliminated from equations (2.2) and (2.3) by using equation (2.9). The non-dimensional ordinary differential equations of steam function and temperature profile are reduced to the following form

$$F^{(iv)} + 2\alpha\, Re\, A(1-\phi)^{2.5}\, F'\, F'' + (4 - (1-\phi)^{2.5}\, D\, Ha^2)\alpha^2\, F'' = 0, \tag{2.10}$$

$$\theta'' + \frac{B\, Ec\, Pr}{C(1-\phi)^{2.5}}\left[4\alpha^2 F'^2 + (F'')^2 + (1-\phi)^{2.5}\, D\, Ha^2\, \alpha^2\, F'^2\right] = 0, \tag{2.11}$$

Here, prime denotes the differentiation with respect to η. The similarity transforms reduce the boundary conditions as follows:

$$F = 1,\ F' = 0,\ \theta = 1 \quad \text{at } \eta = 1$$
$$F = -1,\ F' = 0,\ \theta = 0 \text{ at } \eta = -1 \tag{2.12}$$

Where, $Re = \frac{Q}{2v_f}$ is Reynolds number, $Pr = \frac{(\mu c_p)_f}{\kappa_f}$ is Prandtl number, $Ec = \frac{U_{max}^2}{(c_p)_f T_h}$ is the Eckert number,

$Ha^2 = \frac{\sigma_f B_0^2}{\rho_f \nu_f}$ is square of Hartmann number and α is the channel angle. Moreover,

$$A = (1-\phi) + \frac{\rho_s}{\rho_f}\phi, \qquad B = (1-\phi) + \frac{(\rho c_p)_s}{(\rho c_p)_f}\phi\,,$$

$$C = \frac{\kappa_s + (m+1)\kappa_f - (m+1)(\kappa_f - \kappa_s)\phi}{\kappa_s + (m+1)\kappa_f + (\kappa_f - \kappa_s)\phi},$$

$D = 1 + \left[3\left(\frac{\sigma_s}{\sigma_f} - 1\right)\phi \Big/ \left(\left(\frac{\sigma_s}{\sigma_f} + 2\right) - \left(\frac{\sigma_s}{\sigma_f} - 1\right)\phi\right)\right]$ are the constants.

3. Series Analysis

The non-linear differential equations (2.10) and (2.11) are solved for stream function and temperature profile. To solve equations (2.10) and (2.11), the power series expansions are assumed in terms of the parameter α as follows:

$$F(\eta) = \sum_{i=0}^{\infty} F_i(\eta)\alpha^i, \;\; \theta(\eta) = \sum_{i=0}^{\infty} \theta_i(\eta)\alpha^i, \quad as \;\; |\alpha| < 1 \tag{3.1}$$

By substituting the equation (3.1) into equations (2.10) and (2.11) along with the boundary conditions (2.12) and then equating the coefficient of power of α.

Order zero(α^0):

$$F_0^{(iv)} = 0, \qquad \theta_0'' + \frac{B\ Ec\ Pr}{C(1-\phi)^{2.5}}(F_0'')^2 = 0 \tag{3.2}$$

$$F_0 = 1, F_0' = 0, \theta_0 = 1 \;\; at\ \eta = 1 \tag{3.3}$$

$$F_0 = -1, F_0' = 0, \theta_0 = 0\ at\ \eta = -1 \tag{3.4}$$

Order one(α^1):

$$F_1^{(iv)} + 2\ Re\ A(1-\phi)^{2.5} F_0' F_0'' = 0, \theta_1'' + \frac{B\ Ec\ Pr}{C(1-\phi)^{2.5}}(2F_0''F_1'') = 0 \tag{3.5}$$

$$F_1 = 0, F_1' = 0, \theta_1 = 0\ at\ \eta = 1 \tag{3.6}$$

$$F_1 = 0, F_1' = 0, \theta_1 = 0\ at\ \eta = -1 \tag{3.7}$$

The first 13 coefficients of the series for stream function $F(\eta)$ and temperature $\theta(\eta)$ have been calculated using algebraic programming language MAPLE. The first few coefficients of the series for $F(\eta)$ and $\theta(\eta)$ in terms of $\alpha, Re, Ha, Ec, Pr, \phi, A, B, C, D$ are as follows:

$$F(\eta;\alpha, Re, Ha, \varphi, A, D) = \tfrac{3}{2}\eta - \tfrac{1}{2}\eta^3 - \tfrac{3}{280}\ Re\ A(1-\phi)^{(5/2)}\eta(\eta^2-5)(\eta-1)^2(\eta+1)^2\alpha + \Big(\tfrac{1}{431200}\eta(\eta-1)^2(\eta+1)^2(43120 + 14375\ Re^2\ A^2\ \phi^4 + 28750\ Re^2\ A^2\ \phi^2 - 2875\ Re^2\ A^2\ \phi^5) - 14375\ Re^2\ A^2\ \phi - 28750\ Re^2\ A^2\ \phi^3 - 98\eta^6\ Re^2\ A^2 - 2472\ \eta^2\ Re^2\ A^2 + 954\ \eta^4\ Re^2\ A^2 - 10780\sqrt{1-\phi}\ D\ Ha^2 - 4795\ \eta^4\ Re^2\ A^2\ \phi + 4795\ \eta^4\ Re^2\ A^2\ \phi^4 + 9590\ \eta^4\ Re^2\ A^2\ \phi^2 - 9590\ \eta^4\ Re^2\ A^2\ \phi^3 + 98\ \eta^6\ Re^2\ A^2\ \phi^5 + 490\ \eta^6\ Re^2\ A^2\ \phi^5 - 980\ \eta^6\ Re^2\ A^2\ \phi^2 + 980\ \eta^6\ Re^2\ A^2\ \phi^3 - 490\ \eta^6\ Re^2\ A^2\ \phi^4 - 959\ \eta^4\ Re^2\ A^2\ \phi^5 + 2472\ \eta^2\ Re^2\ A^2\ \phi^5 - 24720\ \eta^2\ Re^2\ A^2\ \phi^2 + 24720\ \eta^2 Re^2\ A^2\ \phi^3 - 12360\ \eta^2\ Re^2\ A^2\ \phi^4 + 12360\ \eta^2\ Re^2\ A^2\ \phi + 21560\ \sqrt{1-\phi}\ D\ Ha^2\ \phi - 10780\ \sqrt{1-\phi}\ D\ Ha^2\ \phi^2\Big)\alpha^2 +$$

$$O(\alpha^3)+\ldots \tag{3.8}$$

$$\theta(\eta;\ \alpha, Re, Ha, \phi, Ec, Pr, A, B, C, D) = -\frac{1}{4C(1-\phi)^{(5/2)}}(1+\eta)\big(3\ B\ Ec\ \mathrm{Pr}\ \eta^3 - 3\ B\ Ec\ \mathrm{Pr}\ \eta^2 + 3\ B\ Ec\ \mathrm{Pr}\ \eta - 2\ C\ (1-\phi)^{(5/2)} - 3\ B\ Ec\ Pr\big) - \frac{3}{560\ C}\ B\ Ec\ \mathrm{Pr}\ Re\ A(9\eta^4 - 38\eta^2 - 19)\ (\eta-1)^2(\eta+1)^2\alpha + O(\alpha^2)+\ldots \tag{3.9}$$

4. Numerical Procedure: Hermite-Padé Approximants

In this present study, a very effective solution method, known as Hermite-Padé approximants, which was first introduced by Padé [26] and Hermite [27] have been applied. In this method, a function is an approximant for the series

$$S_{N-1}(\alpha) = \sum_{n=0}^{N-1} a_n \alpha^n \qquad as \qquad |\alpha| < 1 \tag{4.1}$$

If it shares with S, the similar first few series coefficients for $|\alpha| < 1$. Therefore, the simple approximants are the partial sums of the series S. As soon as this series converges quickly, such polynomial approximants can provide good approximations of the sum.
Consider the $(d+1)$ tuple of polynomials, where d is a positive integer,

$P_N^{[0]}, P_N^{[1]}, \ldots, P_N^{[d]}$

where, $\deg P_N^{[0]} + \deg P_N^{[1]} + \ldots + \deg P_N^{[d]} + d = N,$ (4.2)
is a Hermite-Padé form of these series if

$$\sum_{i=0}^{d} P_N^{[i]}(\alpha) S_i(\alpha) = O(\alpha^N) \quad as \quad |\alpha| < 1 \tag{4.3}$$

Here, $S_0(\alpha), S_1(\alpha), \ldots, S_d(\alpha)$ may be independent series or different form of a unique series. It requires to find the polynomials $P_N^{[i]}$ that satisfy the equation (4.2-4.3). These polynomials are fully determined by their coefficients. Thus, the total number of unknowns in equation (4.3) is

$$\sum_{i=0}^{d} \deg P_N^{[i]} + d + 1 = N + 1 \tag{4.4}$$

Expanding the left hand side of equation (4.3) in powers of α and equating the first N equations of the system equal to zero, we get a system of linear homogeneous equations. To compute the coefficients of the Hermite-Padé polynomials, it requires the normalization form, such as

$$P_N^{[i]}(0) = 1 \ \text{ for some integer } \ 0 \le i \le d \tag{4.5}$$

It is necessary to emphasize that the only input required for the computation of the Hermite-Padé polynomials are the first N coefficients of the series $S_0(\alpha), S_1(\alpha), \ldots, S_d(\alpha)$. The equation (4.4) simply ensures that the coefficient matrix associated with the system is square. One approach to construct the Hermite-Padé polynomials is to solve the system of linear equations using any standard method such as Gaussian elimination or Gauss-Jordan elimination.
Drazin and Tourigney [28] approximant is a particular kind of algebraic approximants and Khan [29] introduced High-order differential approximant (HODA) as a special type of differential approximants. Drazin-Tourigney differential approximant is applied to both the series solutions (3.8) and (3.9) to analyse the results. Then, the influence of physical parameters namely channel angle α, Reynolds number *Re*, Hartmann number *Ha*, nanoparticles volume fraction ϕ, Eckert number *Ec* on velocity profiles and temperature distributions with the effect of three different shapes of Cu-nanoparticles is presented in section 5.

5. Results and Discussion

Three different shapes' effects of nanoparticles such as: brick, cylinder and platelet are analysed on velocity profiles and temperature distributions for varying values of physical parameters such as; nanoparticles solid volume friction $\boldsymbol{\phi}$, channel angle $\boldsymbol{\alpha}$, Reynolds number $\boldsymbol{Re}$, Hartmann number $\boldsymbol{Ha}$, Eckert number $\boldsymbol{Ec}$ and Prandtl number $\boldsymbol{Pr}$ in the present study.

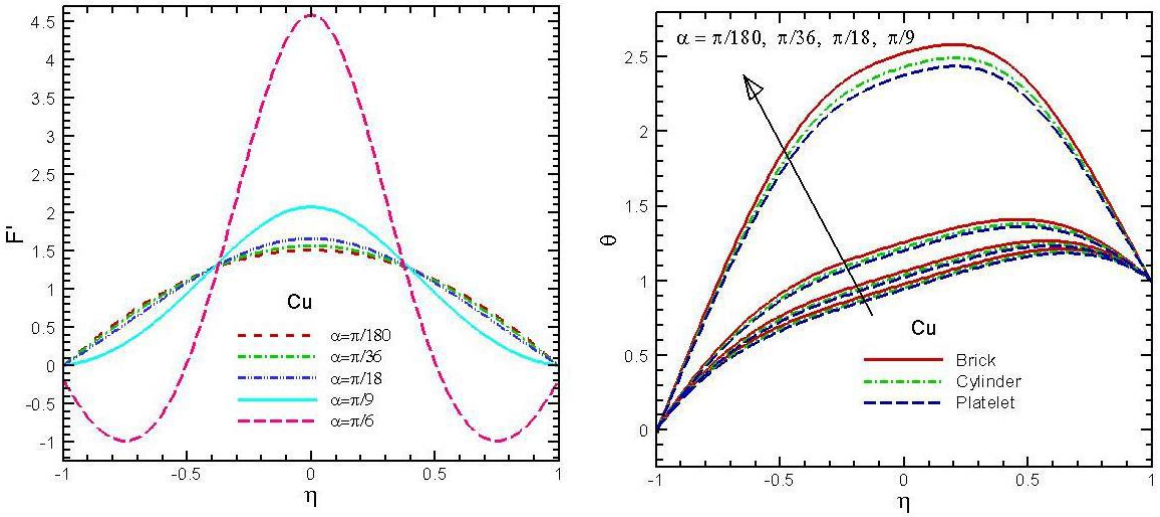

(a) (b)

Fig. 5.1: (a) Velocity Profiles, (b) temperature distributions of Cu –water nanofluid with different values of α at $Re = 10, Ha = 1, \phi = 0.05, Pr = 7.1, Ec = 0.1$.

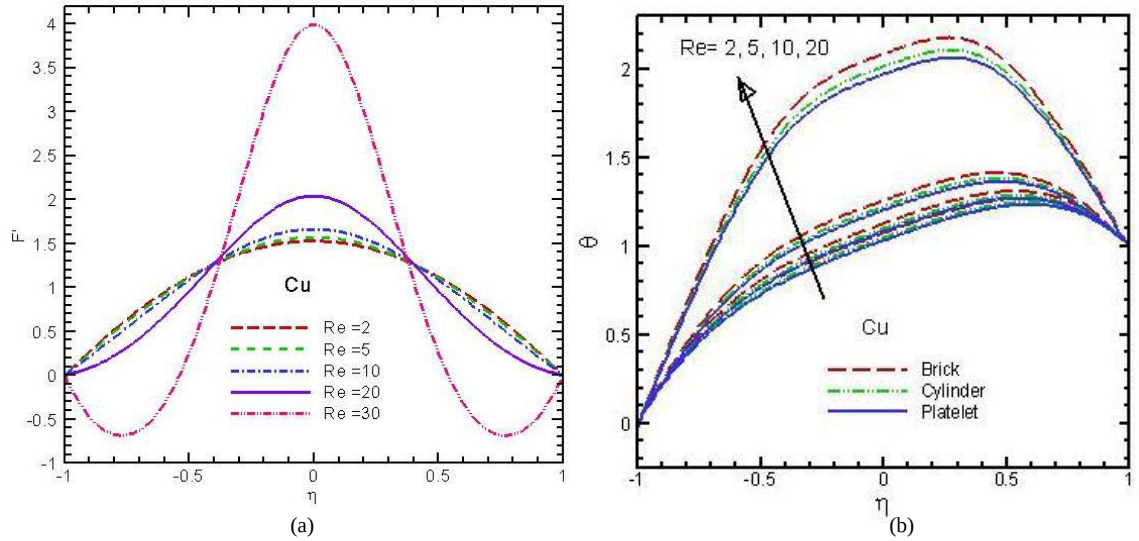

(a) (b)

Fig. 5.2: (a) Velocity Profiles, (b) temperature distributions of Cu–water nanofluid with different values of Re at $\alpha = \pi/18, Ha = 1, \phi = 0.05, Pr = 7.1, Ec = 0.1$.

The channel angle effect on the velocity profiles and temperature distributions for Cu-water nanofluid in the divergent channel is shown in Figs. 5.1(a-b). It is observed in Fig. 5.1 (a) that, the velocity around the centerline increases for the rising values of α. One can also see that the rising values of channel opening α produces backward flow adjacent to the two walls of the channel. Cu –nanoparticle (at $\phi = 0.05$) accelerate the enhancement of centerline velocities more swiftly and there occurs major backward flow near the walls for large value of $\alpha = \pi/6$. It is noticed that if channel opening expands, then exhibited flow generates at the centerline and as a result, a major backward flow raised near the walls for diverging channel. The hypothesis of Fig. 5.1(a) agreed well with those results of Alam et al. [17].

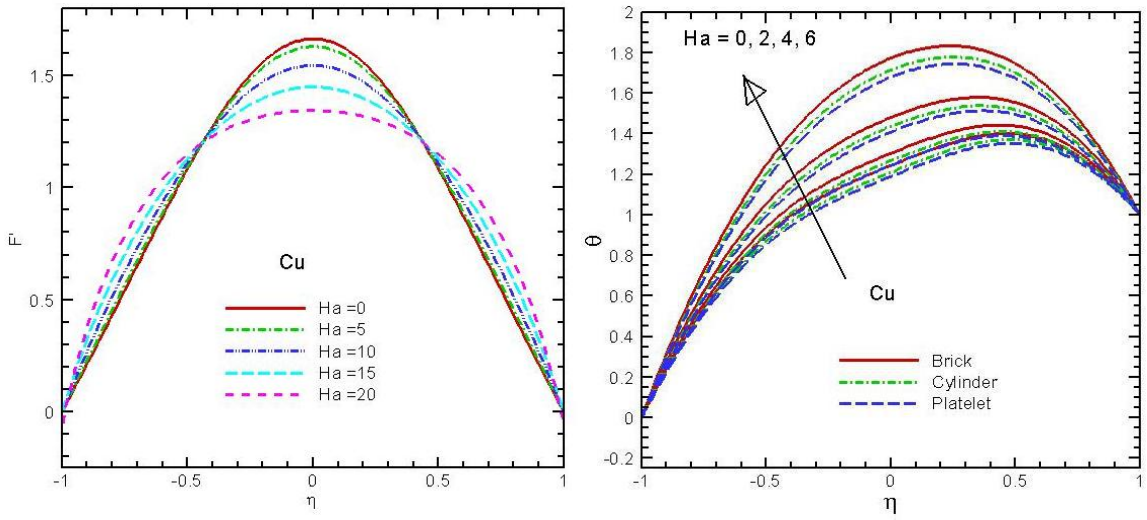

(a) (b)

Fig. 5.3: (a) Velocity Profiles, (b) temperature distributions of Cu–water nanofluid with different values of Ha at $\alpha = \pi/18, Re = 10, \phi = 0.05, Pr = 7.1, Ec = 0.1$.

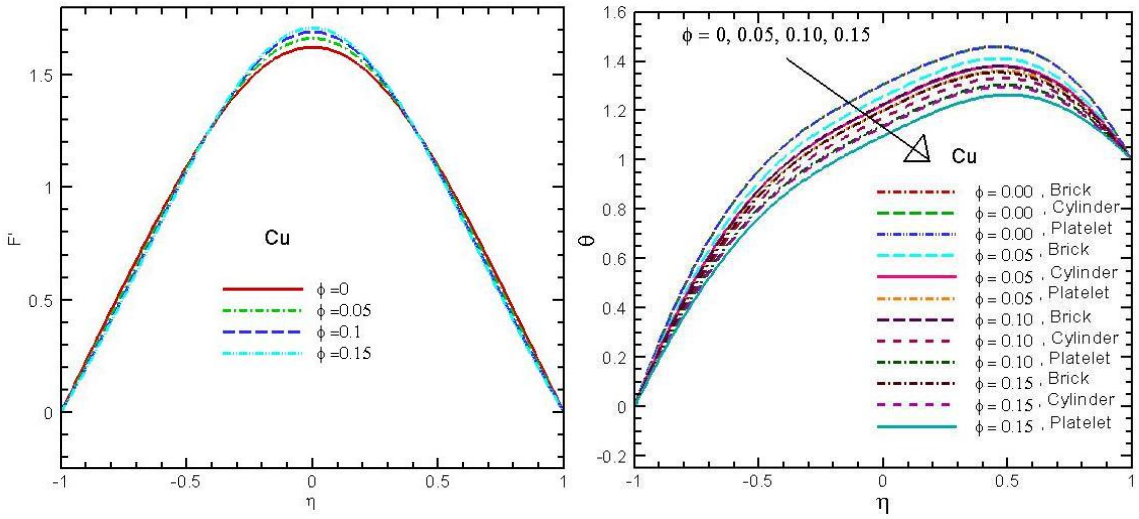

(a) (b)

Fig. 5.4: (a) Velocity Profiles, (b) temperature distributions of Cu–water nanofluid for different values of ϕ at $\alpha = \pi/18,\ Re = 10,\ Ha = 1, Ec = 0.1, Pr = 7.1$.

Figure 5.1(b) represents the effect of channel angle α on temperature profiles. It is noticed that the temperature increases massively around the channel centerline due to the escalating values of channel angle for Cu-nanoparticles. There is almost negligible change in the temperature of the fluid near the walls of the channel. Figures 5.2(a-b) highlight the velocity profiles and temperature distributions of Cu-water nanofluid for the increment of Reynolds number Re. It is interestingly observed in Fig. 5.2(a) that the centerline velocity increases when the value of Re increases, since backward flow arises at the walls. Since Reynolds number is the ratio of momentum forces and the viscous forces. This means that higher values of Re are due to the stronger momentum forces for Cu –water nanofluid. Due to this reason, these forces generate fully developed flow at centerline and an important reverse flow at the channel walls. For increasing values of Re on the variations in temperature are portrayed in Fig. 5.2(b). Since Re is the ratio of momentum forces and viscous forces, it indicates that stronger momentum forces are responsible for rising temperature in divergent channel case. The increasing values of α and Re accelerate the fluid velocity around the channel centerline. These expanded fluid flow produces consistently higher temperature in Figs. 5.1(b) and 5.2(b). It is seen that the brick-shaped nanoparticles have higher temperature followed by cylinder- and platelet- shaped nanoparticles in all incidents.

For a divergent channel, the effects of increasing Hartmann number Ha on the velocity profile and temperature distribution are plotted in Figs. 5.3(a-b). The velocity curves show that the rate of alteration is significantly reduced with increase of Hartmann number. The velocity along the centerline $(-0.5 < \eta < 0.5)$ reduces for the increasing value of Ha. The velocity decreases near the left wall $(-1.0 < \eta < -0.5)$ and right wall $(0.5 < \eta < 1.0)$ uniformly for the decreasing value of Ha. The variation of Ha leads to the variation of the Lorentz force due to magnetic field. This Lorentz force produces more resistance to the alternation phenomena. Figure 5.3(b) demonstrate the effect of Hartmann number on temperature field for Cu–nanoparticles. The higher values of temperature around channel centerline are observed for rising Hartmann number Ha. Near the walls of the channel, there is almost negligible change in the temperature of the fluid. It can be seen that brick –shaped nanoparticles have higher temperature than cylinder – and platelet –shaped nanoparticles.

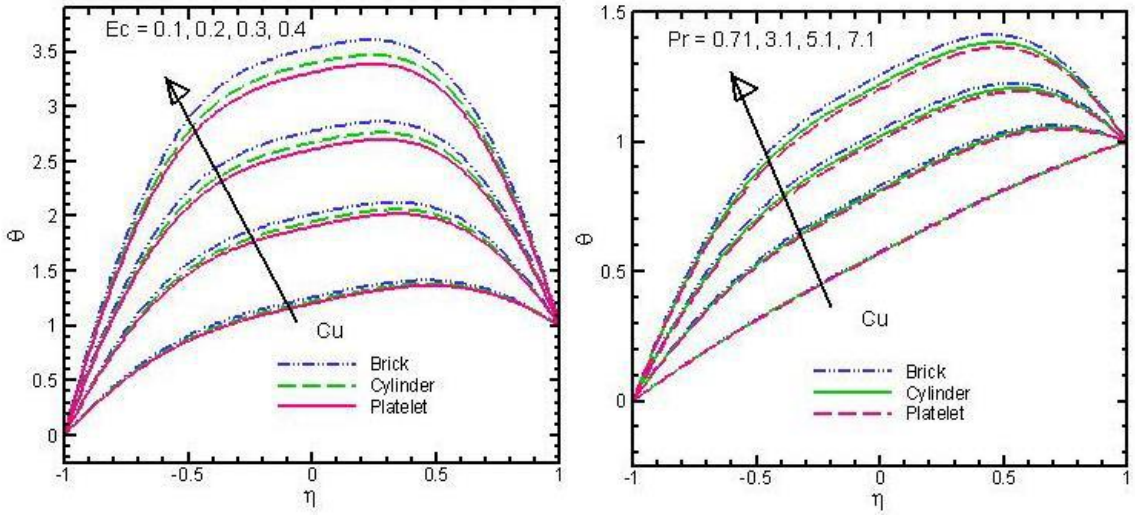

(a) (b)

Fig. 5.5: Temperature profiles of Cu –nanoparticles for different values of (a) Ec and (b) Pr at $\alpha = \pi/18, \phi = 0.05, Re = 10, Ha = 1$.

The effect of solid volume fraction ϕ of Cu -nanoparticles is investigated in the range of $0 \leq \phi \leq 0.15$ with $Ha = 1$ and is displayed in Figs. 5.4(a-b). In Fig. 5.4(a), it is observed that as the solid volume fraction ϕ increases, the velocity increases. The volume fraction ϕ increases when the nanofluids consistency increases and this increasing consistency enhances the fluid flow. For the increasing value of solid volume fraction the velocity expands, but the difference in the velocity is very small. The effects of Cu–nanoparticles solid volume fraction ϕ on temperature distributions with various shape factors are shown in Fig. 5.4(b). It is observed that when the value of ϕ increases, the temperature distribution reduces particularly toward the channel centerline. When $\phi = 0.00$, there is almost negligible change in the temperature of the fluid for three different shaped nanoparticles which is consistent.

Table 5.1: Comparison of the solutions for different number of coefficients of stream function F when $Re = 10, Ha = 1, \alpha = \pi/18, \emptyset = 0.05$

η	$N = 5$	$N = 6$	$N = 7$	$N = 8$	$N = 9$	$N = 10$	$N = 11$	$N = 12$	$N = 13$
-1.0	-1.000000	-1.000000	-1.000000	-1.000000	-1.000000	-1.000000	-1.000000	-1.000000	-1.000000
-0.8	-0.9571418	-0.9571878	-0.9572025	-0.9572074	-0.9572091	-0.9572096	-0.9572098	-0.9572099	-0.9572099
-0.6	-0.8263751	-0.8265170	-0.8265623	-0.8265773	-0.8265824	-0.8265841	-0.8265847	-0.8265850	-0.8265850
-0.4	-0.6105530	-0.6107610	-0.6108278	-0.6108499	-0.6108574	-0.6108600	-0.6108609	-0.6108612	-0.6108614
-0.2	-0.3251298	-0.3252911	-0.3253434	-0.3253608	-0.3253667	-0.3253688	-0.3253695	-0.3253697	-0.3253698
0.0	0.0000000	0.0000000	0.0000000	0.0000000	0.0000000	0.0000000	0.0000000	0.0000000	0.0000000

0.2	0.3251298	0.3252911	0.3253434	0.3253608	0.3253667	0.3253688	0.3253695	0.3253697	0.3253698
0.4	0.6105530	0.6107610	0.6108278	0.6108499	0.6108574	0.6108600	0.6108609	0.6108612	0.6108614
0.6	0.8263751	0.8265170	0.8265623	0.8265773	0.8265824	0.8265841	0.8265847	0.8265850	0.8265850
0.8	0.9571418	0.9571878	0.9572025	0.9572074	0.9572091	0.9572096	0.9572098	0.9572099	0.9572099
1.0	1.0000000	1.0000000	1.0000000	1.0000000	1.0000000	1.0000000	1.0000000	1.0000000	1.0000000

For other values of ϕ, the brick-shaped nanoparticles have highest temperature values compared to cylinder-shaped and platelet-shaped nanoparticles. The effect of Eckert number, Ec on temperature field for Cu – nanoparticles within the channel is discussed in Fig. 5.5(a). We know that Eckert number is the ratio of the square of maximum velocity and specific heat. As a result, it is found from Fig. 5.5(a) that the temperature increases at this region and the fluid flow rate along the centerline becomes faster for increasing values of Eckert number. The effect due to the dissipation term in energy equation is defined by Eckert number. From this figure, it can also be verified that due to the stronger viscous forces, the temperature of the fluid rises in divergent channel. Variations of Prandtl number, Pr on temperature profiles are plotted in Fig. 5.5(b) for Cu-nanoparticles. Rise in temperature for higher values of Prandtl number is observed for Cu–nanoparticles. Prandtl number is the ratio of viscous force and thermal force. Increase of viscosity is responsible for the increasing values of Pr. Thus, the increasing value of temperature distribution of the fluid is seen close to the centerline of the channel. Table 5.1 represents the comparative values of stream function for different numbers of coefficients of the solution (3.8). It is observed that if the number of coefficients in the solution increases from
$N = 5$ to $N = 13$, the values of stream function F increase gradually and uniformly for all values of η.

6. Conclusions

This paper has studied magnetohydrodynamics (MHD) Cu-water nanofluid flow in a divergent channel with the effects of three different shapes of nanoparticles. The influences of different flow parameters on the velocity field and temperature distribution are extensively analysed. The three shapes of nanoparticles are brick, cylinder and platelet –shaped. The major conclusions of this work are as follows:

- The increasing values of α and Re speed up the fluid velocity around the channel centerline and these developd flow produce higher temperature values in this region.
- The fluid velocity lessens while the temperature increases near the channel centerline at greater values of Hartmann number. Besides, fluid flow close the two walls increases as Ha increases.
- The velocity profile rises however the temperature reduces for escalating values of the nanoparticles volume fraction.
- As the values of Eckert number and Prandtl number increased, the temperature distributions around the channel centerline become higher.
- The temperature field inside the channel affected significantly by the nanoparticles shape factors. Brick-shaped nanoparticles have larger temperature values than the cylinder-shaped and platelet-shaped nanoparticles.

Acknowledgements

This work is done within the framework of the Master's program of the second author under Department of Mathematics, Jagannath University, Dhaka.

Funding

Financial support from the National Science and Technology (NST) scholarship is acknowledged.

References

[1] G. B. Jeffery, A viscous fluid of the two dimensional steady motion, *Philosophical Magazine*, 6: 455-465(1915).
[2] G. Hamel, Spiralfo¨rmige Bewgungen Za¨her Flu¨ssigkeiten, *Jahresbericht der Deutschen Math Vereinigung*, 25: 34-60(1916).
[3] Batchelor, K., An introduction to fluid dynamics, Cambridge University Press, Cambridge (1916).
[4] Q. Esmaili, A. Ramiar, E. Alizadeh and D. D. Ganji, An approximation of the analytical solution of the Jeffery-Hamel flow by decomposition method, *Physics Letters A*, 372: 3434-3439 (2008).
[5] R. Sadri, Channel entrance flow. Doctor of Philosophy thesis, Department of Mechanical Engineering, University of Western Ontario (1997).
[6] M. Hamadiche, J. Scott and D. Jeandel, Temporal stability of Jeffery-Hamel flow, *Journal of Fluid Mechanics,* 268: 71 – 88 (1996).
[7] L. Rosenhead, The steady two-dimensional radial flow of viscous fluid between two inclined plane walls, *Proceedings of the Royal Society A*, 175:436 – 467 (1940).
[8] Goldstein, S., Modern developments in fluid mechanics, Clarendon Press: Oxford (1938).
[9] Makinde, O. D., Steady flow in a linearly diverging asymmetrical channel, *Computer Assisted Mechanical and Engineering Sciences*, 4: 157-165 (1997).
[10] S. U. S. Choi, Enhancing thermal conductivity of fluids with nanoparticles, *In proceeding of the 1995 ASME International Mechanical Engineering Congress and Exposition*, 66: 99-105 (1995).
[11] S. K. Das, S. U. S. Choi and W. YU. T. Pradeep, New York: Nanofluids: Science and Technology (2007).
[12] O. D. Makinde and P. Y. Mhone, Hermite-Pade´ Approximation approach to Hydromagnetic flows in convergent-divergent channels, *Applied Mathematics and Computation*, 181: 966-972 (2006).
[13] O. D. Makinde and P. Y. Mhone, Temporal stability of small disturbances in MHD Jeffery-Hamel flows, *Computers and Mathematics with Applications*, 53: 128-136 (2007).
[14] A. Moradi, A. Alsaedi and T. Hayat, Investigation of heat transfer and viscous dissipation effects on the Jeffery-Hamel flow of nanofluids, *Thermal Science*, 19: 563-578 (2015).
[15] Md. S. Alam, M. A. H. Khan and M. A. Alim, Magnetohydrodynamic Stability of Jeffery-Hamel Flow using Different Nanoparticles, *Journal of Applied Fluid Mechanics*, 9: 899-908 (2016).
[16] Md. S. Alam, O. D. Makinde and M. A. H. Khan, Instability of variable thermal conductivity magnetohydrodynamic nanofluid flow in a vertical porous channel of varying width, *Defect and Diffusion Forum*, 378: 85 – 101 (2017).
[17] Md. S. Alam and M. A. H. Khan, Analysis of Magnetohydrodynamic Jeffery- Hamel flow with nanoparticle by Hermite- Padé approximation technique, *International Journal of Engineering Transaction A*, 28: 599 – 607 (2015).
[18] S. Sindhu and B. J. Gireesha, Effect of nanoparticle shapes on irreversibility analysis of nanofluid in a microchannel with individual effects of radiative heat flux, velocity slip and convective heating, *Heat Transfer*, 50: 876-892 (2021).
[19] Asifa, T. Anwar, P. Kumam, Z. Shah and K. Sitthithakerngkiet, Significance of shape factor in heat transfer performance of molybdenum-disulfide nanofluid in multiple flow situations; A comparative fractional study, *Molecules*, 26: 3711 (2021).
[20] A. Bhattad and J. Sarkar, Effects of nanoparticle shape and size on the thermohydraulic performance of plate evaporator using hybrid nanofluids, *Journal of Thermal Analysis and Calorimetry*, 143: 767–779 (2021).
[21] A. C. Das and M. S. Alam, Effect of various shaped Al_2O_3 and TiO_2 nanoparticles on water-based MHD nanofluid flow through convergent-divergent channels, Science & Technology Asia, 26(2): 1-15, (2021).
[22] S. K. Das, S. U. S. Choi and H. E. Patel, Heat transfer in nanofluids- a review, *Heat Transfer Engineering*, 27(10): 3-19 (2006).
[23] R. Ellahi, M. Hassan and A. Zeeshan, Shape effects of nanosize particles in Cu-H_2O nanofluid on entropy generation, *International Journal of Heat Mass Transfer*, 81: 449-456 (2015).
[24] N. Sher Akber and A.W. Butt, Ferromagnetic effects for peristaltic flow of Cu-water nanofluid for different shapes of nanosize particles, *Applied Nanoscience*, Epub Ahead of Print 28 March (2015). DOI: 10.007/s13204-015-0430-x.

[25] R. Ellahi, M. Hasan, A. Zeeshan, The shape effects of nanoparticles suspended in HFE-7100 over wedge with entropy generation and mixed convection, *Applied Nanoscience*, Epub Ahead of print 26 July (2015). DOI: 10.007/s13204-015-0481-z.

[26] H. Padé, Sur Ia repésentation approachée d`une function pour des fractions rationnelles, *Annales Scientifiques del' École Normalle Supérieure,* 9: 1 – 93 (1892).

[27] C. Hermite, Sur Ia générealization des fractions continues algébriques, *Annali di Mathematica Pura e Applicata*, 21: 289-308 (1893).

[28] P.G. Drazin and Y. Tourigny, Numerically study of bifurcation by analytic continuation of a function defined by a power series, *SIAM Journal of Applied Mathematics*, 56: 1 – 18 (1996).

[29] M.A.H. Khan, High-Order Differential Approximants, *Journal of Computational and Applied Mathematics*, 149: 457-468 (2002).